

Selection of Antibody Single-chain Variable Fragments with Improved Carbohydrate Binding by Phage Display*

(Received for publication, September 9, 1993, and in revised form, November 15, 1993)

Su-jun Deng, C. Roger MacKenzie, Joanna Sadowska‡, Joseph Michniewicz, N. Martin Young, David R. Bundle‡, and Saran A. Narang§

From the Institute for Biological Sciences, National Research Council of Canada, Ottawa, Ontario K1A 0R6, Canada

A single-chain variable fragment (Fv) version of a murine monoclonal antibody, Se155-4, specific for *Salmonella* serogroup B O-polysaccharide, was used as a model system for testing monovalent phage display as a route for enhancing the relatively low affinities that typify anti-carbohydrate antibodies. Random single-chain Fv mutant libraries generated by chemical and error-prone polymerase chain reaction methods were panned against the serogroup B lipopolysaccharide. Panning of a randomly mutated heavy chain variable domain library indicated selection for improved serogroup B binders and yielded six mutants, five of which showed wild type activity by enzyme immunoassay. Two of these were apparently selected on the basis of better functional single-chain Fv yield in *Escherichia coli*. A heavy chain mutation (Ile⁷⁷ → Thr) in one mutant, 3B1, appeared to have a particularly dramatic effect, resulting in yields of approximately 120 mg/liter of functional periplasmic product. The sixth mutant, 4B2, had complementarity determining region 1 (CDR1) and CDR2 mutations and demonstrated 10-fold improved binding, by enzyme immunoassay, relative to the wild type. Extensive analysis of antigen-antibody interactions indicated that the improved binding properties of 4B2 were attributable to a higher association rate constant and interaction with an epitope that is larger than the trisaccharide recognized by the wild type. None of the mutations involved known trisaccharide contact residues; this was consistent with analysis of wild type and mutant single-chain Fvs by titration microcalorimetry. Examination of the structure indicated that two mutations in the heavy chain CDR2 provided improved surface complementarity between the protein and the extended epitope encompassing 2 additional hexose residues. However, introduction of only the CDR2 mutations into the wild type structure failed to confer the improved binding properties of 4B2, indicating an indirect effect by the more distant mutations. Panning of randomly mutated light chain variable domain and full-length single-chain Fv mutant libraries did not yield mutants with improved assembly or binding properties.

Intervention in recognition events in which carbohydrates participate has great potential in the prevention and therapy of various disease states because carbohydrates are primary

* This is National Research Council of Canada publication 37373. The costs of publication of this article were defrayed in part by the payment of page charges. This article must therefore be hereby marked "advertisement" in accordance with 18 U.S.C. Section 1734 solely to indicate this fact.

‡ Present address: Dept. of Chemistry, University of Alberta, Edmonton, Alberta T6G 2G2, Canada.

§ To whom correspondence should be addressed. Tel.: 613-990-3247; Fax: 613-941-1327.

markers in cellular recognition processes (1). A major challenge in this area is to overcome the problems associated with the relatively low affinities that are characteristic of most carbohydrate-binding proteins, a trait that also makes them obvious candidates for protein engineering from both theoretical and practical perspectives. We have used an antibody Se155-4, specific for *Salmonella* serogroup B O-polysaccharide, as a model system for investigating the molecular basis of carbohydrate binding by proteins. The advantages offered by this system include a well refined crystal structure (2), a detailed description of binding thermodynamics¹ (3, 4), and an efficient *Escherichia coli* expression system for Fab and single-chain Fv² (5, 6). An extensive site-directed mutagenesis study expanded our understanding of antigen binding by Se155-4 but also showed the limitations of predictive binding site redesign (7). In view of this, *in vitro* mimicry of the immune system, particularly its capacity for diversification under selective pressure, is an attractive alternative to a completely rational approach to redesign. By expressing antibody fragments on the surface of filamentous bacteriophages, it is possible to mimic both the antigen-driven selection and affinity maturation stages of the immune response (8).

In this report we describe the screening of randomly generated mutants of Se155-4 by the phage display technology that has recently been developed for the isolation of antibody fragments by expression of natural (9–11) or semisynthetic (12) variable-gene libraries on bacteriophage surfaces. The entire V_H or V_L domains and full-length scFv were subjected to mutation by chemical and error-prone PCR methods, and the resulting mutant libraries were panned against serogroup B lipopolysaccharide. Only the V_H libraries yielded clones with improved binding to serogroup B lipopolysaccharide. The majority of the amino acid residues that contribute to binding pocket formation and participate in the antigen-antibody hydrogen bond network reside in this domain. However, it is possible that the heavy chain interactions with antigen can be improved since CDRH2, although involved in binding pocket formation, interacts only weakly with the antigen.

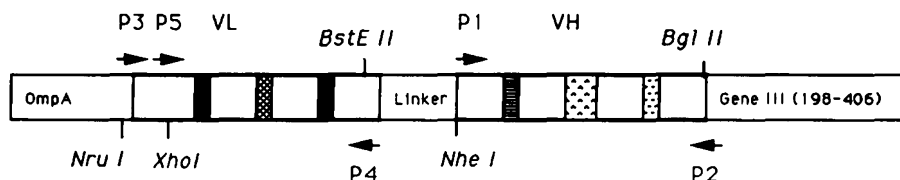
EXPERIMENTAL PROCEDURES

Materials, Strains, and General Methods—All DNA manipulations were carried out by standard procedures (13). *E. coli* strain XL1-Blue and plasmid pBluescript II SK(+) were purchased from Stratagene, and helper phage M13K07 was purchased from Life Technologies, Inc. Serogroup B lipopolysaccharide, O-chain, BSA-antigen conjugates, and

¹ Bundle, D. R., Eichler, E., Gidney, M. A. J., Meldal, M., Ragauskas, A., Sigurskjold, B. W., Sinnott, B., Watson, D. C., Yaguchi, M., and Young, N. M. (1994) *Biochemistry*, in press.

² The abbreviations used are: Fv, variable fragment; BSA, bovine serum albumin; CDR, complementarity-determining region; EIA, enzyme immunoassay; FR3, framework 3 region; PCR, polymerase chain reaction; scFv, single-chain Fv; PAGE, polyacrylamide gel electrophoresis; SPR, surface plasmon resonance; V_L, light chain variable domain; V_H, heavy chain variable domain.

Fig. 1. scFv/gene III fusion showing the restriction sites used for insertion of PCR-amplified V_H , V_L , and full-length scFv products into phagemid pSK4.



trisaccharide methyl glycoside were prepared as described elsewhere.¹ Enzyme conjugates and substrates for immunoassays were obtained from Caltag, Kirkegaard and Perry Laboratories and Bio-Rad.

Construction of scFv-gIII Expression Phagemid—The scFv gene contained in plasmid ptsFvLH(e), which encodes Se155-4 scFv with a V_L - V_H domain orientation with Val¹⁰⁶ of V_L and Glu¹ of V_H linked by a sequence (LGQPKSSPSVTLFPPSSNG) derived from the light chain elbow region (6). The scFv gene was fused to the sequence encoding the carboxyl-terminal domain (Pro¹⁹⁸-Ser⁴⁰⁶) of the filamentous phage gIII protein via a sequence encoding a GGGGS linker (Fig. 1). The linker sequence and gIII fragment from *Bgl*II to *Hind*III were amplified from M13mp18 RF DNA by PCR using primers 5'-GCGAGATCTGGTGGCG-TGGATCCCATTGCTTTGTGAATATCAA-3' and 5'-AACAGCTTCTAATAATAACGGAATACCCAAAAGAAGCTGG-3'. The PCR product was digested with *Bgl*II and *Hind*III and ligated with *Bgl*II-*Hind*III large fragment of ptsFvLH(e) (6). The resulting plasmid was digested with *Pvu*II, and the fragment containing scFv-gIII was ligated with the *Pvu*II large fragment of pBluescript II SK (+). The insertion orientation was confirmed by *Hind*III-*Nae*I digestion. Expression of scFv-gIII on the surface of phage was confirmed by sodium dodecyl sulfate-polyacrylamide gel electrophoresis/Western blot analysis of phage particles using a goat anti-mouse λ -chain antibody conjugated to alkaline phosphatase. The phagemid expressing the highest level of fusion protein was used as wild type scFv-gIII construct for mutation studies and was designated as pSK4.

Library Construction and Panning—Random mutagenesis using plasmid pSK4 as the template was performed by error-prone PCR (50 cycles) under conditions that reduce the fidelity of DNA synthesis by Taq DNA polymerase (14) and by standard PCR using pSK4 template that was mutated by treating with nitrous acid for 50 min at 24 °C. The basic protocol for random chemical mutagenesis was described earlier (15, 16). Both error-prone PCR and PCR-mediated chemical mutagenesis were carried out using primer 1 (5'-TAAATGAGCTGCAAAGC-TAGCGGTTAC-3'), primer 2 (5'-ACCTCCAGATCTGGAGCTAACGG-TCAGGCTCGCGCCCTG-AC-3'), primer 3 (5'-AAAACCGCTATCG-CGATCGCACTTGCCTGGCTGGTTTCGCTACCGTTGCGGACGGCC-3'), primer 4 (5'-TCGGCGGGAACAGGGTAACCGACGGGC-3'), and primer 5 (5'-GTTACCTGACCTGCCGCTCGAGCAC-3'). For generation of V_H , V_L , and full-length scFv libraries, the reverse-forward primer combinations were 1-2, 3-4, and 5-2, respectively. PCR products were purified by phenol extraction followed by restriction enzyme digestion. The restriction sites used for PCR product digestion and ligation of the PCR products into plasmid pSK4 were *Nhe*I-*Bgl*II, *Nru*I-*Bst*EII, *Xho*I-*Bgl*II, for the V_H , V_L , and full-length scFv libraries, respectively (Fig. 1). For panning, the error-prone PCR and chemical V_H libraries were kept separate while the V_L and full-length single-chain Fv libraries were pooled.

All ligation products were electroporated into *E. coli* XL1-Blue resulting in 5×10^5 transformants from the error-prone PCR approach and 10^6 from the chemical mutagenesis approach. After electroporation, cells were grown in 5 ml of SOC medium for 1 h, 10 ml of SB (35 g/liter tryptone, 20 g/liter yeast extract, 5 g/liter NaCl) containing 50 μ g/ml ampicillin, 75 μ g/ml tetracycline, and 250 μ l of M13K07 (10^{12} plaque-forming units/ml) for 1 h and transferred to 100 ml of SB containing 100 μ g/ml ampicillin and 75 μ g/ml tetracycline. Following overnight growth at 37 °C, cultures were centrifuged, and phage present in the supernatant was harvested by the polyethylene glycol precipitation protocol (17). All displayed libraries were panned against serogroup B lipopolysaccharide, which was coated on microtiter plates at a concentration of 10 μ g/ml. Microtiter plates were washed 40 times with phosphate-buffered saline to remove nonbinders, and binders were eluted from the washed plate with 0.1 M sodium acetate buffer, pH 2.8, containing 0.5 M NaCl. Eluants were immediately neutralized and phage particles in the eluants prepared for the next panning round by amplification in *E. coli* as described above. Five rounds of panning were carried out with each library.

Screening and Sequencing of Clones—After the final round of panning, 50 clones were randomly picked from each library. Microtiter plate cultures (200 μ l) of the selected clones were grown overnight in SB at

30 °C. Following centrifugation, the cells were resuspended in lysis buffer (50 mM Tris, pH 8, containing 150 mM NaCl, 5 mM MgCl₂, 400 μ g/ml lysozyme, and 1 unit/ml DNase) and maintained at room temperature for 1 h. Cell debris was sedimented, and the supernatants were assayed by indirect EIA with microtiter plates coated with 10 μ g/ml serogroup B lipopolysaccharide. Selected clones were also assayed for antigen binding activity by a colony lift procedure essentially the same as that described by Barbas *et al.* (9). After removal of adhering colonies, filters were blocked with 4% BSA in phosphate-buffered saline for 1 h. Filters were then rocked sequentially with (i) 10 μ g/ml O-chain antigen and 1% BSA in phosphate-buffered saline for 1 h; (ii) 1 μ g/ml Se155-5 IgG and 1% BSA in phosphate-buffered saline for 1 h; (iii) protein A/alkaline phosphatase conjugate for 30 min followed by development with appropriate enzyme substrates. All steps were carried out at room temperature. Results obtained with the enzyme-linked immunosorbent assay and colony lift methods were in good agreement.

Clones showing the highest activity in the screening procedures were sequenced by the dideoxy method using a double-stranded DNA cycle sequencing kit (Life Technologies, Inc.) with 5'-CGATTGGCCTT-GATATTCACAAAGC-3' and 5'-TGCGAGCGTTAAAATGAGCTGCC-3' as primers.

Site-directed Mutagenesis—PCR mutagenesis was used to construct the Asn⁵⁵ → Ser/Ser⁵⁶ → Gly double mutant (SG) and to introduce the Ile⁷⁷ → Thr mutation into 4B2 giving a mutant that was designated 4B2/3B1. Mutant SG was constructed by two rounds of PCR. With B-50 Fab (7) as the template, the first introduced the Asn⁵⁵ → Ser/Ser⁵⁶ → Gly double mutation using 5'-ATGGATCGGCGCAATCTATCCGGG-TAGCGGCGC-GACCTTCTACAACC-3' as the upstream primer and 5'-ACCATGGCCACCACGCGTGCAGTAG-3' as the downstream primer. With the first round product as template, a second round introduced an *Eag*I site, for insertion of the mutant sequence into pSK4, with the upstream primer 5'-CAAACAGCGCCGGTTCAGGGTCTAGAATGG-ATCGGCGCAATCTATC-3' and the downstream primer used in round 1. Mutant 4B2/3B1 was constructed using 4B2 as the template with the upstream primer 5'-GCTGTTACTAGTACCACCACCGCTACATG-3' and P2 used in V_H library construction as the downstream primer. Both mutants were confirmed by DNA sequencing.

Production and Isolation of Soluble scFv—Mutants selected for further study were digested with *Bgl*II for insertion of three termination codons between the scFv and gIII sequences by ligation of the linearized plasmids with the self-complementary terminator sequence 5'-GATCT-TAATAGTGATCACTATTAA-3'. Plasmids encoding wild type and mutant scFvs were transformed into *E. coli* strain TG-1 for production of soluble scFv. Clones were grown overnight at 30 °C in M-9 minimal medium containing 0.4% casamino acids (1-liter cultures) prior to induction with isopropyl-1-thio- β -D-galactopyranoside and supplementation with additional nutrients as described previously (6). Functional scFv was isolated from periplasmic extracts by affinity chromatography as described previously except that an elution buffer of lower pH, 0.1 M sodium acetate, pH 2.8, containing 0.5 M NaCl, was required with some of the mutants. For mass verification, wild type and mutant scFvs were dialyzed against 5% acetic acid and analyzed by electrospray mass spectrometry on an API III Sciex instrument.

Immunoassay and SPR Analyses—Wild type and mutant scFvs were compared by indirect EIA using plates coated with 10 μ g/ml BSA-trisaccharide or BSA-O-chain. Bound antibody fragment was detected with an anti- λ -chain antibody conjugated to alkaline phosphatase (5). Association rate and dissociation rate constants for the interaction of purified scFv fragments with BSA-antigen conjugates were determined by SPR (18) on a BIAcore™ biosensor system (Pharmacia LKB Biotechnology Inc. Biosensor AB). Immobilizations were carried out using the amine coupling kit supplied by the manufacturer. BSA-trisaccharide and BSA-O-chain were immobilized in 10 mM sodium acetate, pH 4.5, at concentrations and contact times that yielded about 200 resonance units of immobilized material. One resonance unit corresponds to an immobilized protein concentration of ~1 μ g/mm² (19). All measurements were performed at ambient temperature in 10 mM HEPES, pH 7.4, 100 mM NaCl, 3.3 mM EDTA at a flow rate of 5 μ l/min. Surfaces were regenerated with 10 mM HCl. Binding constants were calculated from

TABLE I
Amino acid differences from wild type of heavy chain mutants selected from chemical (series 3B) and PCR (series 4B) generated libraries and of site-directed mutants

scFv type and clone	Position							
	31 ^a	55 ^b	56 ^b	69	77	85	103 ^c	109
Wild type								
SK4	N	N	S	K	I	S	Y	G
Phage display mutants								
3B1					T			
3B5							H	S
3B8			N					
4B2	D	S	G	R		G		S
4B8				N				S
4B21	D				N			
Site-directed mutants								
SG		S	G					
4B2/3B1	D	S	G	R	T	G		S

^a CDR1.

^b CDR2.

^c CDR3.

the association rate and dissociation rate constants using BIAlogue™ software (Pharmacia Biosensor AB).

Titration Microcalorimetry—The thermodynamics of antigen binding by selected mutants were determined using a Microcal Inc. (Northampton, MA) titration microcalorimeter (20). Single-chain Fvs at concentrations of approximately 100 μ M in 50 mM Tris, pH 8, containing 150 mM NaCl were titrated with a 2 mM solutions of trisaccharide antigen in the same buffer at 25 °C. Thermogram data obtained with 20 injections of 5 μ l were analyzed as described previously (3, 4).

RESULTS

Library Generation and Panning—Chemical and error-prone PCR techniques were selected as methods for constructing mutant scFv libraries. The objective was to introduce diversity throughout the gene without generating structural diversity that exceeded the practical limits of library size and the screening process. The monovalent display mode afforded by the phagemid/helper phage system (9, 21) was chosen for screening purposes in the expectation that it would select primarily on the basis of affinity. The size of the error-prone PCR V_H library was estimated to be 5×10^5 , and that of the other libraries was estimated to be 10^6 in each instance. With all libraries, colony-forming unit counts indicated approximately 50-fold enrichment for serogroup B binders during the panning process.

Analysis of Panned Libraries—Serogroup B binders obtained by the enrichment process were screened by enzyme-linked immunosorbent assay and colony lift methods. Based on screening results for the V_H library, 29 clones were sequenced. Only one clone gave the wild type amino acid sequence. The remainder yielded the six mutant sequences shown in Table I. The chemical and error-prone PCR libraries each generated three of the mutant sequences. Sequencing of selected clones from the panned V_L and full-length scFv libraries revealed that all had the 3B1 or 4B2 sequences shown in Table I. It was obvious that these clones were contaminants from the V_H library because they carried the same silent mutations as these clones.

There was a surprisingly strong bias toward substitutions at certain positions with all six V_H mutants. All exhibited substitutions at one or more of residues 31, 55, 56, 77, and 109 (Table I). Mutations appeared at four CDR positions, three FR3 positions, and one FR4 position. Particularly striking were the FR4 mutation, Gly¹⁰⁹ \rightarrow Ser, which occurred in three of the six mutants and the CDR1 mutation, Asn³¹ \rightarrow Asp, which occurred in half of the mutants. Mass spectrometry was used as a convenient and accurate means of confirming the expected masses of wild type and mutant molecules. All observed values fell within a range of 4–6 Da above the calculated masses (calculated molecular mass = 26,547 for the wild type).

Single-chain Fv Yields—Product yields obtained by affinity

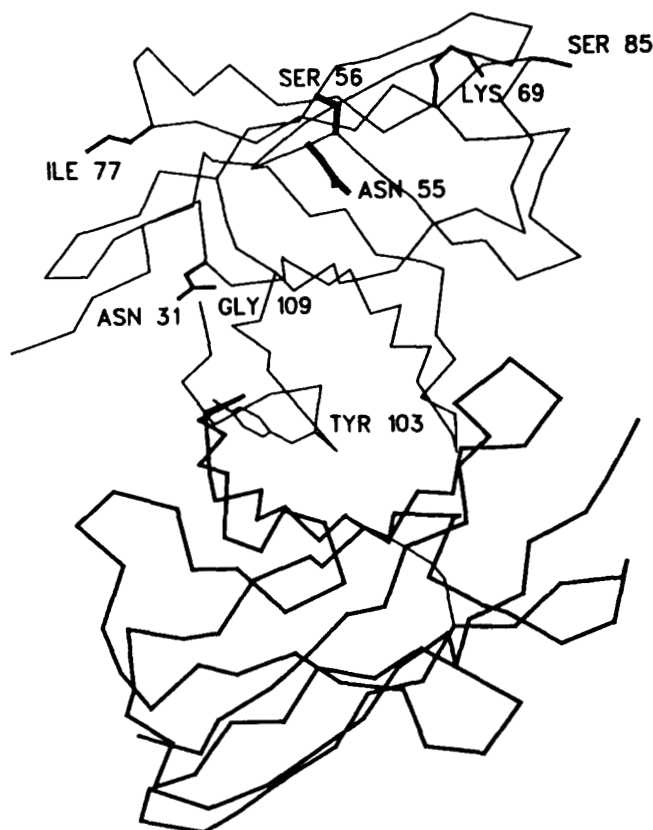


FIG. 2. Se155-4 Fv α -carbon backbone showing the wild type side chains at positions exhibiting substitutions in the six V_H mutants. The light chain backbone is shown in bold. The view is one looking down into the binding pocket. In its bound state, the antigen lies approximately perpendicular to the V_H-V_L interface.

chromatography and indirect EIA analysis of periplasmic extracts indicated that at least two of the mutants were selected on the basis of increased yield of functional scFv. In particular, replacement of Ile⁷⁷ by Thr or Asn appeared to be associated with increased yield. Whereas the wild-type construct typically gave yields of active product in the 10–15 mg/liter range, mutants 3B1, with an Ile⁷⁷ \rightarrow Thr mutation and 4B21, with an Ile⁷⁷ \rightarrow Asn, mutation, gave yields of approximately 120 and 50 mg/liter of soluble periplasmic scFv, respectively.

Structural Interpretation—With the exception of the position 109 mutations, substitutions were limited to FR3 and the CDR1 and CDR2 loops (Fig. 2). Ile⁷⁷, an FR3 residue that is solvent-exposed, was replaced by Asn in two of the six mutants

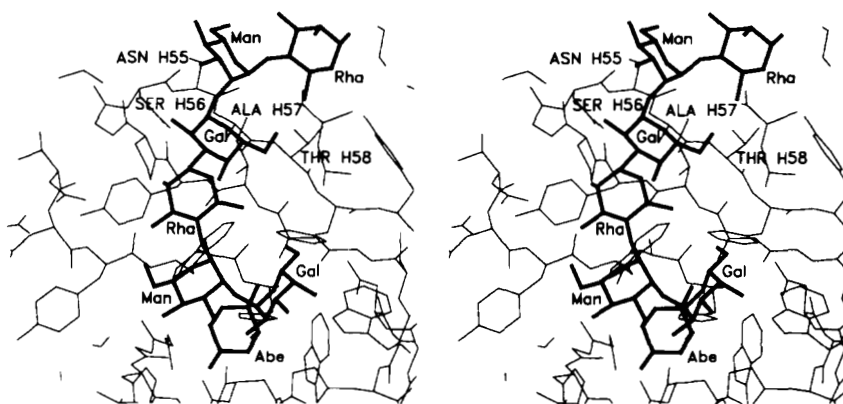


FIG. 3. Stereo drawing of the antigen-antibody complex showing the region where unfavorable contacts exist between the wild type heavy chain CDR2 loop and the extended epitope. The antigen is a heptasaccharide in which the abequeose has been removed from the second repeating unit.

and Thr in a third. There was a strong bias for Asn³¹ → Asp and Gly¹⁰⁹ → Ser mutations, but reasons for these preferences were not apparent. Although Asn³¹ is a heavy chain CDR1 residue, it is not within antigen contact distance (Fig. 3).

The CDRH2 substitutions in mutant 4B2 are in an area where in the absence of conformational changes the extended oligosaccharide epitope clashes with the wild type structure. The Asn⁵⁵ → Ser and Ser⁵⁶ → Gly mutations appeared to improve surface complementarity between the protein and the extended epitope encompassing two additional hexoses (rhamnose and galactose), although Ala⁵⁷ still clashes with the galactose moiety of the extended epitope (Fig. 3).

Immunoassay and SPR Analyses—Indirect EIA performed on plates coated with BSA-trisaccharide and BSA-*O*-chain indicated that, of the six mutants described in Table I, only 4B2 exhibited improved antigen binding characteristics. Assays employing BSA-trisaccharide (Man-[Abe]-Gal) and BSA-*O*-chain ((Man-t[Abe]-Gal-Rha)_n) showed that 4B2 binding to these antigens was approximately 10-fold higher in each instance, relative to the wild type (Fig. 4). Affinity chromatography elution conditions also showed enhanced binding by 4B2. Although wild type scFv eluted from an *O*-chain antigen column at pH 4.5, more acidic conditions were required for 4B2 elution. Of the other five mutants, four showed EIA activity that was similar to that of the wild type (data not shown), whereas 3B1 displayed slightly weaker activity, particularly on BSA-*O*-chain plates (Fig. 4).

SPR analyses (Table II) of representative mutants generally agreed well with the EIA results. Relative to the wild type, 4B2 displayed approximately 10-fold stronger affinity for BSA-trisaccharide, ($K_a = 4.5 \times 10^7 \text{ M}^{-1}$ compared with $6.0 \times 10^6 \text{ M}^{-1}$ for the wild type) and BSA-*O*-chain, whereas 3B8 and 4B21 displayed similar affinities, and 3B1 showed slightly weaker binding (K_a values = $3.1 \times 10^6 \text{ M}^{-1}$ and $1.5 \times 10^6 \text{ M}^{-1}$ with the trisaccharide and *O*-chain conjugate, respectively). The improved binding properties of 4B2 were entirely attributable to a higher association rate constant ($k_{on} = 1.3 \times 10^5 \text{ M}^{-1} \text{ s}^{-1}$ compared with $1.2 \times 10^4 \text{ M}^{-1} \text{ s}^{-1}$ for the wild type with the trisaccharide conjugate). The dissociation rates were quite similar, although the k_{off} values for 4B2/3B1 and 4B21 ($3.4 \times 10^{-3} \text{ s}^{-1}$ and $3.7 \times 10^{-3} \text{ s}^{-1}$, respectively, with the trisaccharide conjugate) were approximately twice as fast as that of the wild type and other mutants (Table II, Fig. 5). There was a striking difference in the association profile of 4B2 compared with that of the wild type and other mutants (Fig. 5). Whereas the 4B2 association phase with BSA-trisaccharide and BSA-*O*-chain was classical, that of the other mutants and the wild type was distinctly biphasic. When sensorgrams showed biphasic binding, the association

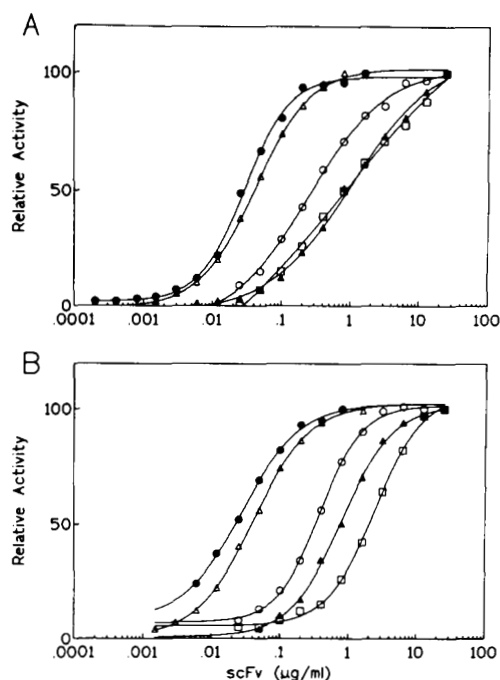


FIG. 4. Indirect enzyme immunoassay showing the binding of wild type and mutant scFvs to BSA-trisaccharide (A) and BSA-*O*-chain (B). ○, wild type; △, 4B2; □, 3B1; ●, 4B2/3B1; ▲, SG. Bound antibody was detected with an anti- λ -chain/alkaline phosphatase conjugate.

rate constants were calculated using the slower second phase.

Site-directed Mutants—A site-directed mutant was constructed to analyze the contribution of the CDRH2 mutations to improved antigen binding by 4B2. Surprisingly this mutant (SG), with Asn⁵⁵ → Ser and Ser⁵⁶ → Gly mutations displayed an antigen binding profile characterized by biphasic binding to both BSA-trisaccharide and BSA-*O*-chain and affinity, $K_a = 9.0 \times 10^6 \text{ M}^{-1}$ with the trisaccharide conjugate, that more closely resembled wild type than 4B2 activity.

A site-specific mutant was also constructed to determine the additive effects of introducing the mutations thought to be responsible for the high 3B1 yield and enhanced 4B2 binding in the same scFv. The resulting scFv showed better binding than 4B2 in immunoassays (Fig. 4), but SPR results indicated very similar kinetics (Table II).

Thermodynamic Analyses—In contrast to the immunoassay and biosensor results, titration microcalorimetry showed that the affinities of wild type ($K_a = 1.3 \times 10^6 \text{ M}^{-1}$) and 4B2 ($K_a = 1.0$

TABLE II
Affinities and kinetics of BSA-trisaccharide and BSA-O-chain binding by wild type and mutant scFvs

scFv	BSA-trisaccharide			BSA-O-chain		
	k_{on} $M^{-1} s^{-1}$	k_{off} s^{-1}	K_a M^{-1}	k_{on} $M^{-1} s^{-1}$	k_{off} s^{-1}	K_a M^{-1}
Wild type	1.2×10^4	2.0×10^{-3}	6.0×10^6	1.9×10^4	4.0×10^{-3}	4.8×10^6
4B2	1.3×10^5	2.9×10^{-3}	4.5×10^7	1.5×10^5	3.8×10^{-3}	4.0×10^7
3B1	4.6×10^3	1.5×10^{-3}	3.1×10^6	8.2×10^3	5.5×10^{-3}	1.5×10^6
3B8	1.3×10^4	1.6×10^{-3}	8.1×10^6	1.7×10^4	3.1×10^{-3}	5.5×10^6
SG	1.8×10^4	2.0×10^{-3}	9.0×10^6	1.9×10^4	4.1×10^{-3}	4.6×10^6
4B2/3B1	1.7×10^5	3.4×10^{-3}	5.0×10^7	1.7×10^5	5.7×10^{-3}	3.0×10^7
4B21	1.4×10^4	3.7×10^{-3}	3.8×10^6	2.4×10^4	8.5×10^{-3}	2.8×10^6

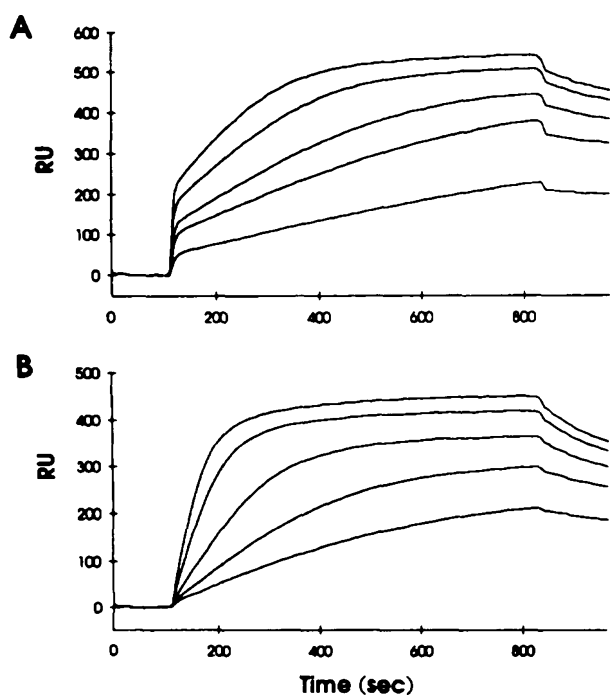


FIG. 5. SPR sensorgrams showing biphasic (A) and monophasic (B) binding of scFvs to immobilized BSA-trisaccharide. In the biphasic example, mutant 3B8 was assayed at concentrations of 100, 200, 300, 500, and 700 nM. In the monophasic example mutant 4B2/3B1 was assayed at concentrations of 10, 20, 40, 80, and 120 nM. The faster k_{off} rate for 4B2/3B1, relative to 3B8, is evident in the sensorgrams.

$\times 10^5 M^{-1}$) for trisaccharide were similar, although the thermodynamics of binding had changed considerably (Table III). Unconjugated trisaccharide was used in calorimetric measurements. Also, mutant 3B1 displayed a binding constant that was as high as 4B2. The 2-amino acid extension to the phage version of the scFv did not affect antigen binding activity. The wild type and mutant forms were characterized by an enthalpy-entropy compensation effect previously observed with mutant Fabs of this antibody (7) and well documented for anti-fluorescyl antibodies (22).

DISCUSSION

Using mutant libraries that were generated as described here, phage display of antibody fragments provided an excellent means of fine tuning Se155-4 for better antigen binding properties and compatibility with the *E. coli* secretory process. By introducing mutations at relatively low frequencies, the error-prone PCR and chemical modification methods introduced subtle structural changes that did not alter the key features of antigen binding. Instead, the libraries yielded structures characterized by enhanced interaction with the extended carbohydrate epitope and with improved functional antibody yield in *E. coli*.

The observation that the phage display system selected for mutants which assembled more efficiently in *E. coli* is of general interest and has practical implications. The functional secretion in *E. coli* of foreign proteins, including antibody fragments, is often problematic, and the underlying reasons that govern success or failure are not understood. Changes at certain positions in the scFv mutants described here may be related to improved folding or better interactions with the linker. Replacement of Ile⁷⁷ in the V_H, a hydrophobic FR3 solvent-exposed residue, by either Asn or Thr resulted in substantially increased yields of functional scFv, suggesting that mutation to a nonhydrophobic residue at this position increases the productive folding of such constructs. The Gly¹⁰⁹ → Ser mutation appears to allow for the formation of hydrogen bonds from Ser OH to the carbonyl oxygen of heavy chain residue 4 and the NH of heavy chain residue 6. The latter 2 residues form a β bulge, and the additional hydrogen bonds may stabilize the structure in the region where the linker approaches the V_H domain.³

Se155-4 binds a trisaccharide epitope within the four-sugar repeating unit of the O-polysaccharide in a "pocket"-like site via a network of hydrogen bonds and van der Waals contacts (2). None of the contact points that confer recognition of this epitope was altered in 4B2, the mutant with the improved binding characteristics described here. The finding that it is difficult to change the fundamental characteristics of antigen binding by Se155-4 is in agreement with an earlier saturation mutagenesis study of heavy chain CDR3 (7), the major participant in the hydrogen bond network.

It is thought that the main reason for improved antigen binding by mutant 4B2 relates to its ability to accommodate more easily an extended carbohydrate epitope because of reduced surface bulk in the heavy chain CDR2 region. However, the binding properties of the site-directed SG mutant indicated that this explanation is incomplete and that the 4B2 mutations which are more remote from the combining site also exert indirect effects that are partially responsible for the 4B2 binding properties. The observation that mutants 3B8 and 4B21, which contain some of the 4B2 mutations not associated with heavy chain CDR2, do not exhibit enhanced binding also supports the idea that the 4B2 mutations act in concert to produce the properties of this mutant. The indirect influence of noncontact residues on antigen binding has been reported for several other antibodies and appears to be a general phenomenon. In a site-directed mutagenesis study, Sharon (23) showed synergistic interactions between mutations that resulted in a 200-fold enhancement in affinity of an anti-*p*-azophenylarsonate antibody. Also, in an analysis of somatic mutations in an anti-lysozyme antibody, Lavoie *et al.* (24) observed that mutations involving residues not contacting antigen enhanced binding by indirect or long range effects. If the improved binding displayed by 4B2 is primarily related to a reduction of antigen-antibody steric clashes in the heavy chain CDR2 region, this would lead to

³ A. Zdanov, Y. Li, D. R. Bundle, S.-J. Deng, C. R. MacKenzie, S. A. Narang, N. M. Young, and M. Cygler, submitted for publication.

TABLE III
Thermodynamic parameters for trisaccharide binding by Se155-4 Fab, scFv, and heavy chain scFv mutants isolated by phage display

	K	ΔG°	ΔH°	$-\Delta S^\circ$
	M^{-1}		$kJ\ mol^{-1}$	
<i>E. coli</i> wild type Fab	$2.1 \pm 0.3 \times 10^5$	-30.3 ± 0.4	-24.8 ± 0.6	-5.5 ± 0.7
Wild type scFv	$1.3 \pm 0.5 \times 10^5$	-29.1 ± 0.9	-23.7 ± 1.0	-5.4 ± 1.8
Extended wild type scFv ^a	$1.3 \pm 0.2 \times 10^5$	-29.1 ± 0.4	-28.5 ± 1.2	-0.5 ± 1.3
3B1 scFv ^a	$1.1 \pm 0.2 \times 10^5$	-28.8 ± 0.4	-31.1 ± 0.8	2.3 ± 0.9
4B2 scFv ^a	$1.0 \pm 0.1 \times 10^5$	-28.7 ± 0.3	-37.4 ± 1.0	8.7 ± 1.1

^a The positioning of termination codons between the scFv and gene III sequences resulted in an Arg-Ser carboxyl-terminal extension.

improved binding of larger oligosaccharides or trisaccharide conjugates but not of the trisaccharide hapten itself. The thermodynamic data support this interpretation since the mutants show very little change in the binding constants for the trisaccharide ligand. In contrast, the EIA and SPR analyses with the BSA-trisaccharide and BSA-polysaccharide conjugates show a far greater range of mutant properties. With the BSA-trisaccharide conjugate, the BSA or the nine-carbon tether may still clash with the heavy chain CDR2 region, in the manner of the O-chain.

Anti-carbohydrate antibodies have not been extensively studied from the standpoint of antigen binding kinetics, but the evidence to date indicates that their relatively low affinities are largely attributable to slow on-rates. The association rates reported here, and elsewhere for an antibody specific for a pneumococcal polysaccharide (25), are in the 10^4 – $10^5\ M^{-1}\ s^{-1}$ range and are at least 100-fold slower than those reported for most antigen-antibody systems (26). For the wild type and mutant scFvs described here, the association constants determined by SPR analyses of binding kinetics were considerably greater than those from the thermodynamic data for the trisaccharide. For the wild type protein, the increase was 60-fold and for the 4B2 and 4B2/3B1 mutants 400-fold. Although both techniques give direct interaction data, the microcalorimetry is thermodynamically more accurate, whereas the SPR and EIA systems more closely resemble the natural cell-surface state of carbohydrate antigens. Differences between binding in solid phase and solution assays are frequently observed, and this difference has been a recurring theme in the evaluation of EIA methods to determine K_a (27). The effect of immobilization tends to be an increase in binding constant since less entropy loss will be associated with binding to an immobilized ligand.

Two aspects of these results are of particular biological relevance. First, the monovalent fragments showed significantly higher binding to the immobilized multivalent BSA conjugates, which resemble the natural antigen presentation, than the trisaccharide hapten. The low K_a values often associated with anti-carbohydrate antibodies are largely from experiments with such haptens, and these may have generally underestimated the binding affinities of these antibodies. Second, the mutations undoubtedly increased k_{on} , and there is growing evidence that this parameter has particular biological significance. In a study of the maturation response to oxazolone, Foote and Milstein (28) observed a kinetic selection that resulted in a shift of antibody repertoire toward a population with high k_{on} rates. Also, Lawrence and Springer (29) proposed that endothelial selectin molecules that mediate the initial interaction with carbohydrate ligands on neutrophils during inflammation are selected on the basis of rapid k_{on} rates and not affinity.

Although phage display is an excellent tool for the selection and amplification of rare mutant proteins, success in isolating structures with desired functional properties ultimately depends on the molecular composition of the library that is displayed. Although the library generation approaches used here worked well for Se155-4 fine tuning, they would not be suitable for all applications. For example, preliminary attempts at iso-

lating *Salmonella* serogroup A and D binders from such libraries have not been successful. The construction of libraries in which mutations are restricted to the CDRs may be more useful in this regard and is being developed for Se155-4 (30).

Acknowledgments—We thank Anne Webb for assistance with the titration microcalorimetry, Doris Bilous for synthesizing deoxyoligonucleotides, and Dr. Eleonora Altman for preparing and supplying affinity matrix and the antigen-BSA conjugates. We are grateful to Dr. Steven Evans for preparation of the stereo diagram. Thanks are also due to Dr. Bob Reed (Pharmacia Biosensor AB) and Suzanne Grothé and Dr. Maureen O'Connor (Biotechnology Research Institute, N. R. C.) for help with the SPR analyses. This is NRCC publication no. 37373.

REFERENCES

- Drickamer, K., and Carver, J. (1992) *Curr. Opin. Struct. Biol.* **2**, 653–654
- Cyglar, M., Rose, D. R., and Bundle, D. R. (1991) *Science* **253**, 442–445
- Sigurskjöld, B. W., Altman, E., and Bundle, D. R. (1991) *Eur. J. Biochem.* **197**, 239–246
- Sigurskjöld, B. W., and Bundle, D. R. (1992) *J. Biol. Chem.* **267**, 8371–8376
- Anand, N. N., Dubuc, G., Phipps, J., MacKenzie, C. R., Sadowska, J., Young, N. M., Bundle, D. R., and Narang, S. A. (1991) *Gene (Amst.)* **100**, 39–44
- Anand, N. N., Mandal, S., MacKenzie, C. R., Sadowska, J., Sigurskjöld, B., Young, N. M., Bundle, D. R., and Narang, S. A. (1991) *J. Biol. Chem.* **266**, 21874–21879
- Brummell, D. A., Sharma, V. P., Anand, N. N., Bilous, D., Dubuc, G., Michniewicz, J., MacKenzie, C. R., Sadowska, J., Sigurskjöld, B. W., Sinnott, B., Young, N. M., Bundle, D. R., and Narang, S. A. (1993) *Biochemistry* **32**, 1180–1187
- Marks, J. D., Hoogenboom, H. R., Griffiths, A. D., and Winter, G. (1992) *J. Biol. Chem.* **267**, 16007–16010
- Barbas, C. F., Kang, A. S., Lerner, R. A., and Benkovic, S. J. (1991) *Proc. Natl. Acad. Sci. U. S. A.* **88**, 7978–7982
- Marks, J. D., Hoogenboom, H. R., Bonnett, T. P., McCafferty, J., Griffiths, A. D., and Winter, G. (1991) *J. Mol. Biol.* **222**, 581–597
- McCafferty, J., Griffiths, A. D., Winter, G., and Chiswell, D. A. (1990) *Nature* **348**, 552–554
- Barbas, C. F., Bain, J. D., Hoekstra, D. M., and Lerner, R. A. (1992) *Proc. Natl. Acad. Sci. U. S. A.* **89**, 4457–4461
- Sambrook, J., Fritsch, E. F., and Maniatis, T. (1989) *Molecular Cloning: A Laboratory Manual*, 2nd Ed., Cold Spring Harbor Laboratory, Cold Spring Harbor, NY
- Leung, D. W., Chen, E., and Goeddel, D. V. (1989) *J. Methods Cell. Mol. Biol.* **1**, 11–15
- Diaz, J.-J., Rhoads, D. D., and Roufa, D. J. (1991) *BioTechniques* **11**, 204–211
- Myers, R. M., Lerman, L. S., and Maniatis, T. (1985) *Science* **229**, 242–247
- Cwirla, S. E., Peters, E. H., Barrett, R. W., and Dower, W. S. (1990) *Proc. Natl. Acad. Sci. U. S. A.* **87**, 6378–6382
- Jönsson, U., Fägerstam, L., Ivarsson, B., Johnsson, B., Karlsson, R., Lundh, K., Löfås, S., Persson, B., Roos, H., Rönnberg, I., Sjölander, S., Stenberg, E., Ståhlberg, R., Urbaniczky, C., Östlin, H., and Malmqvist, M. (1991) *BioTechniques* **11**, 620–627
- Stenberg, E., Persson, B., Roos, H., and Urbaniczky, C. (1991) *J. Colloid Interface Sci.* **143**, 513–526
- Wiseman, T., Williston, S., Brandts, J. F., and Lin, L.-N. (1989) *Anal. Biochem.* **17**, 131–137
- Bass, S., Greene, R., and Wells, J. A. (1990) *Proteins Struct. Funct. Genet.* **8**, 309–314
- Herron, J. N., Kranz, D. M., Jameson, D. M., and Voss, E. W. (1988) *Biochemistry* **25**, 4602–4609
- Sharon, J. (1990) *Proc. Natl. Acad. Sci. U. S. A.* **87**, 4814–4817
- Lavoie, T. B., Drohan, W. N., and Smith-Gill, S. J. (1992) *J. Immunol.* **148**, 503–513
- Maeda, H., Schmidt-Kessen, A., Engel, J., and Jatón, J.-C. (1977) *Biochemistry* **16**, 4086–4089
- Pecht, I. (1982) *Aspects Antibody Funct.* **6**, 1–68
- Azimzadeh, A., Pellequer, J. L., and Van Regenmortel, M. H. V. (1992) *J. Mol. Recognit.* **5**, 9–18
- Foote, J., and Milstein, C. (1991) *Nature* **352**, 530–532
- Lawrence, M. B., and Springer, T. A. (1991) *Cell* **65**, 859–873
- Deng, S.-j., MacKenzie, C. R., and Narang, S. A. (1993) *Nucleic Acids Res.* **21**, 4418–4419